Polyhedron 187 (2020) 114665

Contents lists available at ScienceDirect

Polyhedron

journal homepage: www.elsevier.com/locate/poly

Synthesis, structure and *in vitro* anticancer activity of Pd(II) complexes of mono- and *bis*-pyrazolyl-*s*-triazine ligands

Jamal Lasri [a,*], Hessa H. Al-Rasheed [b], Ayman El-Faham [b,c,*], Matti Haukka [d], Nael Abutaha [e], Saied M. Soliman [c,*]

[a] Department of Chemistry, Rabigh College of Science and Arts, King Abdulaziz University, P.O. Box 344, Jeddah, Saudi Arabia
[b] Department of Chemistry, College of Science, King Saud University, P.O. Box 2455, Riyadh 11451, Saudi Arabia
[c] Department of Chemistry, Faculty of Science, Alexandria University, P.O. Box 426, Ibrahimia, Alexandria 21321, Egypt
[d] Department of Chemistry, University of Jyväskylä, P.O. Box 35, FI-40014 Jyväskylä, Finland
[e] Bioproducts Research Chair, College of Science, Department of Zoology, King Saud University, P.O. Box 2455, Riyadh 11451, Saudi Arabia

ARTICLE INFO

Article history:
Received 2 May 2020
Accepted 5 June 2020
Available online 11 June 2020

Keywords:
Pd(II) complexes
Pyrazolyl-*s*-triazine
Hirshfeld
DFT
Anticancer activity

ABSTRACT

The square planar complexes [Pd(MPT)Cl_2] (**1**) and [Pd(BPT)Cl]ClO_4 (**2**) were synthesized by the reaction of the 4,4′-(6-(3,5-dimethyl-1*H*-pyrazol-1-yl)-1,3,5-triazine-2,4-diyl)dimorpholine (**MPT**) and *N*-methyl-*N*-phenyl-4,6-di(1*H*-pyrazol-1-yl)-1,3,5-triazin-2-amine (**BPT**) ligands with $PdCl_2$ (1:1) in acetone under thermal conditions, respectively. In complex **1**, the Pd(II) ion is coordinated with the **MPT** ligand as a bidentate *NN*-chelate, augmented with two chloride ligands in *cis* positions. In complex **2**, the Pd(II) ion is coordinated with the **BPT** ligand as a tridentate *N*-chelate in a pincer fashion, together with one chloride ligand. Hirshfeld analysis indicated that complex **1** is packed with a significant quantity of Cl…H (20.2%), O…H (6.8–8.1%) and N…H (10.8–11,7%) hydrogen bonds, as well as some C—H…π (8.1–9.0%) interactions and C…O contacts (1.1–2.0%). On the other hand, O…H (13.8%), C—H…π (16.5%) and anion-π stacking (C…O: 1.2%) are the most important interactions in **2**. The atoms in molecules topological parameters correlate well with the Pd-N distances. *In vitro* anticancer experiments showed that both complexes have higher activity than their free ligands against MDA-MB-231 and MCF-7 cell lines. Complex **2** showed the highest cytotoxic activity with IC_{50} = 13.5 and 18.6 μg/mL against MDA-MB-231 and MCF-7, respectively, compared to 30.5 μg/mL for complex **1**.

1. Introduction

Since the remarkable success of cisplatin, carboplatin and oxaliplatin in the treatment of cancer [1], significant efforts have been made to develop new Pt(II) complexes and their Pd(II) analogues, in order to find alternative drugs that combine the strong mode of action with low dose and limited toxicity [2,3]. The use of cisplatin, carboplatin and oxaliplatin drugs for cancer treatment is limited by serious toxicity problems [4–6]. Palladium is a good replacement for platinum in the development of metal-based anticancer drugs [7–11]. Pd(II) complexes are closely related to their Pt (II) analogues due to their structural similarities in coordination chemistry. Since the reported studies by Graham *et al.* [12], which indicated the use of Pd(II) complexes as possible anticancer agents, several novel Pd(II) complexes have been reported with promising anticancer activity. In several cases, the Pd(II) complexes showed better antitumor activity than their Pt(II) counterparts (such as cisplatin, carboplatin, etc.) [11].

On the other hand, the *s*-triazine scaffold affords the basis for the synthesis of numerous compounds with widespread applications in medicinal chemistry [13]. Especially, *s*-triazines bearing a pyrazolyl moiety (Fig. 1), have low toxicity towards growth-stimulating activity [14]. Additionally, they show good anticancer activity [15–17]. Many pyrazolyl-*s*-triazine derivatives showed moderate to strong cytotoxicity depending on the nature of substituent attached to the triazine ring [17]. Recently, a series of *s*-triazine derivatives have been reported that show strong anticancer activities against two human breast cancer cell lines (MCF-7 and MDA-MB-231). It was found that the substituent on the *s*-triazine core showed a significant effect on the anticancer activity [18].

* Corresponding authors at: Department of Chemistry, Rabigh College of Science and Arts, King Abdulaziz University, P.O. Box 344, Jeddah, Saudi Arabia (J. Lasri); Department of Chemistry, College of Science, King Saud University, P.O. Box 2455, Riyadh 11451, Saudi Arabia (A. El-Faham) and Department of Chemistry, Faculty of Science, Alexandria University, P.O. Box 426, Ibrahimia, Alexandria 21321; Egypt (S. M. Soliman).

E-mail addresses: jlasri@kau.edu.sa (J. Lasri), aelfaham@ksu.edu.sa (A. El-Faham), saied1soliman@yahoo.com (S.M. Soliman).

https://doi.org/10.1016/j.poly.2020.114665
0277-5387/

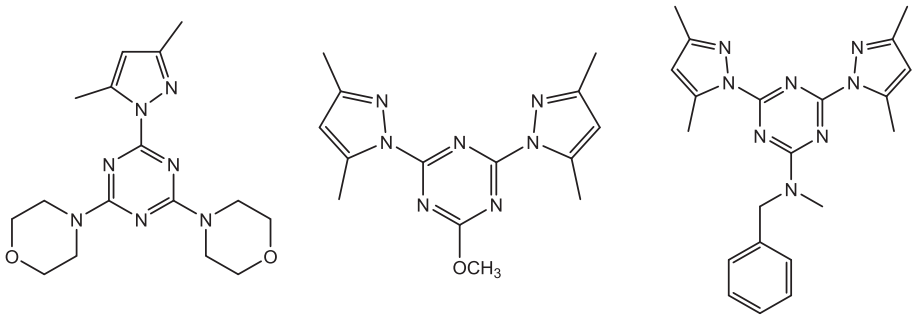

Fig. 1. Structures of the **MPT**, **MBPT** and **BPT** ligands.

From another point of view, Zn(II) and Co(II)-**MBPT** (**MBPT** = 2,4-*bis*(3,5-dimethyl-1*H*-pyrazol-1-yl)-6-methoxy-1,3,5-triazine) [19] and Ag(I)-**MPT** [20] complexes showed a broad spectrum of antimicrobial activities, while Ni(II)-**MBPT** complexes showed selective actions against Gram-positive bacteria [21]. The attractive *bio*-activity of *s*-triazines and their metal complexes, as well as the interesting anticancer activities of pyrazolyl-*s*-triazines [16], triggered us to report herein the synthesis and structure of Pd(II) complexes with the **BPT** and **MPT** ligands (Fig. 1). Additionally, the anticancer activities of the studied Pd(II) complexes compared to their free ligands against breast cancer MCF-7 and MDA-MB-231 cell lines are also discussed.

2. Experimental

2.1. Materials and physical measurements

Chemicals and solvents were purchased from the Sigma-Aldrich Company. The C, H and N analyses were determined using a Perkin-Elmer 2400 elemental analyzer. A JEOL spectrometer (400 MHz) was used to measure the NMR spectra at room temperature in DMSO d_6.

2.2. Syntheses of the ligands and their Pd(II) complexes

2.2.1. Syntheses of the MPT and BPT ligands

The two ligands **MPT** and **BPT** (Fig. 1) were prepared following the reported methods [16,22]. Further experimental details regarding the preparation and characterization of these ligands are available in the Supplementary data.

2.2.2. Synthesis of [Pd(MPT)Cl_2] (**1**)

To a solution of the 4,4′-(6-(3,5-dimethyl-1*H*-pyrazol-1-yl)-1,3,5-triazine-2,4-diyl)dimorpholine (**MPT**) ligand (60.0 mg, 0.174 mmol) in acetone (20 mL) was added $PdCl_2$ (30.8 mg, 0.174 mmol), and the reaction mixture was heated at 50 °C under stirring for 3 days. After that, the mixture was filtered off and kept at room temperature for slow evaporation to afford the final complex [Pd(MPT)Cl_2] (**1**) as orange block crystals.

Yield: 90%. ^{1}H NMR (DMSO d_6) δ, ppm: 2.11 (s, 3H, CH_3), 2.49 (s, 3H, CH_3), 3.56–3.69 (m, 16H, 8 CH_2), 6.05 (s, 1H, C*H*). ^{13}C NMR (DMSO d_6) δ, ppm: 12.3 (*C*H$_3$), 15.6 (CH$_3$), 43.3 (*C*—N—*C*, morpholine), 65.9(*C*—O—*C*, morpholine), 112.4 and 142.5 (*C* = CH, pyrazole), 149.5 (*C*(CH$_3$) = N, pyrazole), 162.7, 164.2, 164.8 (*N*-*C*=N, triazine). Anal. Calcd for $C_{16}H_{25}Cl_2N_7O_3Pd$: C, 35.54; H, 4.66; N, 18.13. Found: C, 35.76; H, 4.35; N, 18.32%.

2.2.3. Synthesis of [Pd(BPT)Cl]ClO_4 (**2**)

To a solution of the *N*-methyl-*N*-phenyl-4,6-di(1*H*-pyrazol-1-yl)-1,3,5-triazin-2-amine (**BPT**) ligand (60.0 mg, 0.154 mmol) in acetone (20 mL) was added $PdCl_2$ (27.3 mg, 0.154 mmol), and the reaction mixture was heated at 50 °C under stirring for 3 days. After that, the mixture was filtered off and kept at room temperature for slow evaporation to afford the final complex [Pd(BPT)Cl]ClO_4 (**2**) as yellow block crystals.

Yield: 91%. ^{1}H NMR (DMSO d_6) δ, ppm: 2.51 (s, 6*H*, 2CH$_3$), 2.62 (s, 3*H*, CH$_3$), 2.74 (s, 3*H*, CH$_3$), 3.29 (s, 3*H*, C*H*$_3$N), 5.02 (s, 2H, C*H*$_2$-Ph), 6.64 (s, 1H, C*H*), 6.68 (s, H, C*H*), 7.37–7.38 (m, 5H, Ph). ^{13}C NMR (DMSO d_6) δ, ppm: 12.3 (CH$_3$), 15.6 (CH$_3$), 40.5 (*C*H$_3$N), 53.5 (CH$_2$Ph), 112.4 (CH = C, pyrazole), 127.1, 128.1, 129.1, 142.5 (C_{ar}), 145.8 (*C*(CH$_3$) = CH, pyrazole), 149.5 (*C*(CH$_3$) = N, pyrazole), 162.7, 164.2, 164.8 (*N*-*C*=N, triazine). Anal. Calcd for $C_{21}H_{24}Cl_2N_8O_4Pd$: C, 40.05; H, 3.84; N, 17.79. Found: C, 40.27; H, 3.99; N, 17.82%.

2.3. Crystal structure determination

The crystal structures of **1** and **2** were measured using a Bruker Kappa Apex II diffractometer using Mo Kα radiation. *Denzo-Scalepack* [23a] was used for cell refinements and data reductions while *SHELXT* software [23b] was used to solve the structures (see

Table 1
Crystal data for complexes **1** and **2**.

	1	**2**
CCDC	1,998,456	1,998,457
Empirical formula	$C_{16}H_{25}Cl_2N_7O_3Pd$	$C_{21}H_{24}Cl_2N_8O_4Pd$
Fw	540.73	629.78
temp (K)	170(2)	170(2)
λ (Å)	0.71073	0.71073
cryst syst	Triclinic	Monoclinic
space group	$P^{-}1$	$P2_1/c$
a (Å)	9.22380(10)	9.9407(2)
b (Å)	9.7348(2)	20.1738(8)
c (Å)	12.4921(2)	12.1803(5)
α (deg)	89.3900(10)	90
β (deg)	85.5100(10)	91.103(2)
γ (deg)	66.0530(10)	90
V (Å^3)	1021.71(3)	2442.21(15)
Z	2	4
ρ_{calc} (Mg/m^3)	1.758	1.713
μ(Mo Kα) (mm^{-1})	1.204	1.025
No. reflns.	20,717	26,364
Unique reflns.	5474	5604
GOOF (F^2)	1.074	1.123
R_{int}	0.0270	0.0823
R1[a] ($I \geq 2\sigma$)	0.0286	0.0753
wR2[b] ($I \geq 2\sigma$)	0.0625	0.1281

[a] $R1 = \Sigma||F_o| - |F_c||/\Sigma|F_o|$. [b] $wR2 = [\Sigma[w(F_o^2 - F_c^2)^2]/\Sigma[w(F_o^2)^2]]^{1/2}$.

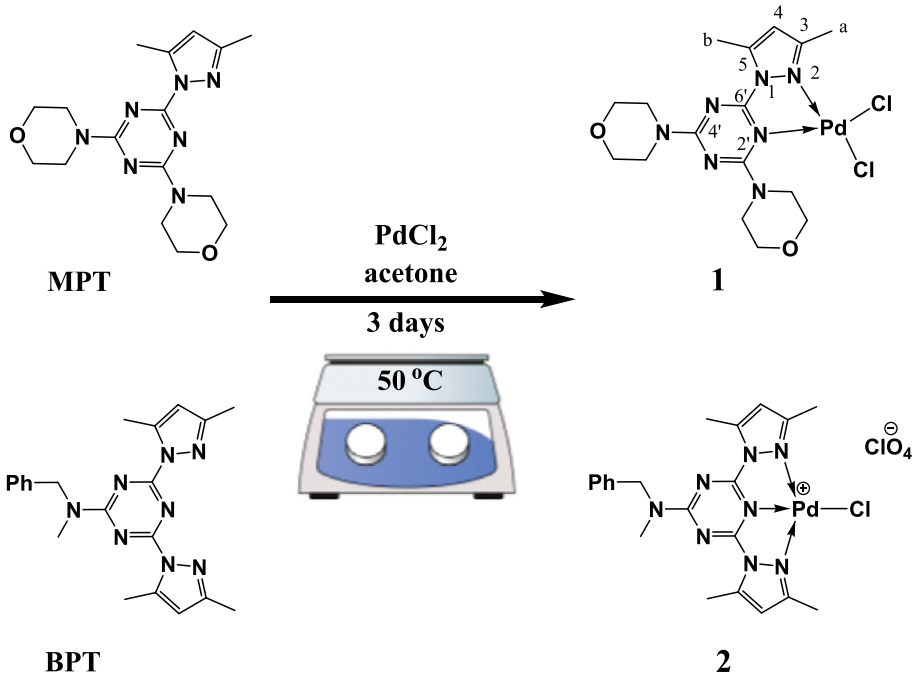

Scheme 1. Synthesis of the $[Pd(MPT)Cl_2]$ (**1**) and $[Pd(BPT)Cl]ClO_4$ (**2**) complexes.

Supplementary data). *SHELXL* software [23b] was used for structural refinements and *SADABS* [23c] for absorption correction (Table 1). Different intermolecular interactions were analyzed using the Crystal Explorer 17.5 program [24].

3. DFT calculations

Using the Gaussian 09 software package [25], single point calculations using MPW1PW91 and Wb97XD methods [26] combined with cc-PVTZ and cc-PVTZ-PP [27] basis sets for non-metal atoms and the Pd atom, respectively were performed. Natural bond orbital and atoms in molecules (AIM) analyses were performed using NBO 3.1 [28] and Multiwfn [29] programs, respectively.

4. *In vitro* anticancer activity

In vitro anticancer activities against two breast adenocarcinoma cell lines were examined. Details regarding the cell lines and cytotoxicity assays are described in the Supplementary data. To study the morphology of MDA-MB-231 and MCF-7 cells, the cells were treated with complex **2** and compared with the control (methanol). Cells were cultured in 24-well plates and exposed to 15 and 20 µg/mL of complex **2** for 48 h. The morphological changes were imaged (20x magnification) using a phase contrast microscope (Leica, Germany).

5. Results and discussion

5.1. Syntheses and characterizations of *1* and *2*

The new Pd(II) complexes $[Pd(MPT)Cl_2]$ (**1**) and $[Pd(BPT)Cl]ClO_4$ (**2**) were synthetized, respectively, by the reaction of **MPT** and **BPT** with $PdCl_2$ (1:1) in acetone under thermal conditions (Scheme 1). Complexes **1** and **2** were characterized by ^1H and ^{13}C NMR spectroscopies, elemental analyses and also by single crystal X-ray diffraction.

The ^1H NMR spectrum of the complex $[Pd(MPT)Cl_2]$ (**1**) showed the two methyl groups of the pyrazolyl moiety (*b* and *a*, Scheme 1) as two singlet peaks at δ 2.11 and 2.49 ppm, respectively, and these

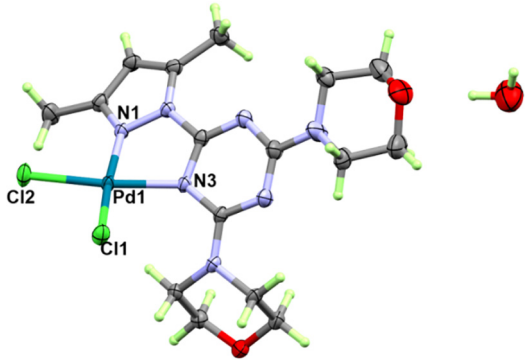

Fig. 2. X-ray structure of **1**.

Table 2
Geometric parameters (Å and °) for **1** and **2**.

Bond	Distance	Bonds	Angles
Complex 1			
Pd1-N1	2.0199(16)	N1-Pd1-N3	78.15(6)
Pd1-N3	2.0595(16)	N1-Pd1-Cl2	96.34(5)
Pd1-Cl2	2.2746(5)	N3-Pd1-Cl2	174.06(5)
Pd1-Cl1	2.2778(5)	N1-Pd1-Cl1	169.91(5)
		N3-Pd1-Cl1	96.30(5)
		Cl2-Pd1-Cl1	88.81(2)
Complex 2			
Pd1-N3	1.929(5)	N3-Pd(1)-N1	78.0(2)
Pd1-N(1	2.038(6)	N3-Pd1-N5	79.1(2)
Pd1-N5	2.046(5)	N1-Pd(1)-N(5)	157.1(2)
Pd1-Cl1	2.2903(18)	N3-Pd1-Cl1	179.61(16)
		N1-Pd1-Cl1	102.36(16)
		N5-Pd1-Cl1	100.57(15)

Table 3
Hydrogen bond parameters (Å and °) for **1** and **2**.

D-H...A	d(D-H)	d(H...A)	d(D...A)	<(DHA)
Complex 1				
C3-H3...Cl1[i]	0.95	2.67	3.470(2)	142.8
O3-H3A...O1	0.98	1.97	2.933(7)	167.4
O3-H3B...Cl2[ii]	0.97	2.34	3.301(3)	172.8
[i]1 x + 1,y,z; [ii] -x + 1,-y + 1,-z				
Complex 2				
C2-H2A...O3#1	0.98	2.59	3.210(9)	121.4
C3-H3...O4 #2	0.95	2.54	3.452(9)	161.1
C20-H20...O3 #3	0.95	2.46	3.299(10)	147.2
[i] −1 + x,y,z; [ii]1-x,1-y,-z ; [iii] 2-x,1-y,-z				

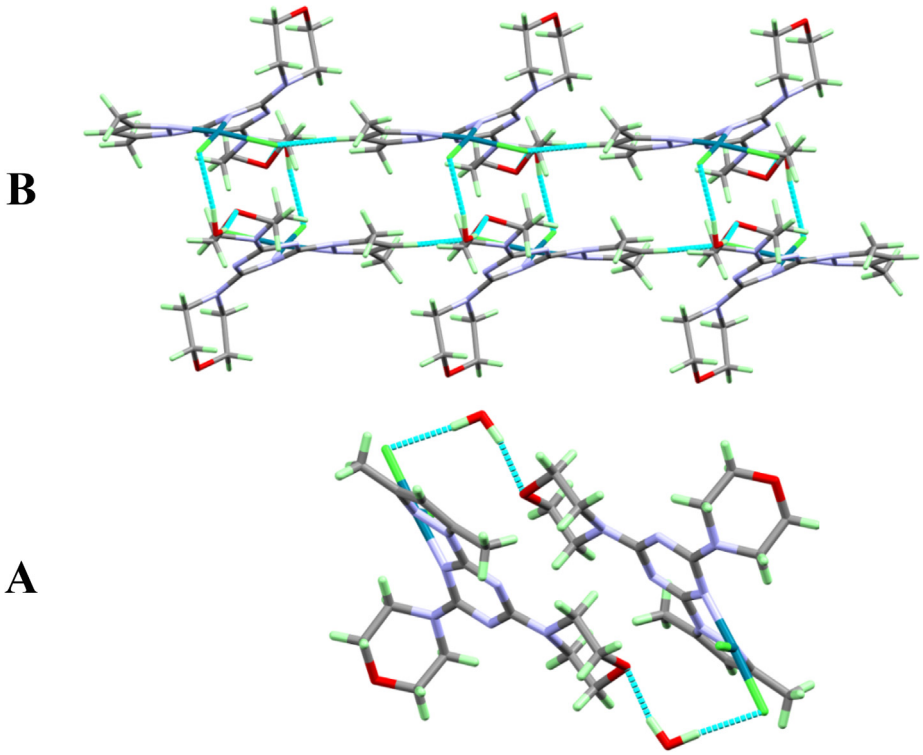

Fig. 3. The hydrogen bonding interactions in the [Pd(MPT)Cl_2] complex (**1**).

were shifted upfield compared to the free ligand (δ 2.27 and 2.59 ppm, respectively). The four methylene groups of the morpholine residue appeared as a multiplet peak in the range δ 3.56–3.69 ppm, while the four methylene groups in the free ligand appeared as a triplet peak at δ 3.17 ppm and a broad singlet at δ 3.82 ppm. The C*H* unit of the pyrazole ring (H_4, Scheme 1) in complex **1** was observed as a singlet peak at δ 6.05 ppm, with a slight downfield shift compared to the free ligand (δ 5.97 ppm). The ^{13}C NMR spectrum of complex **1** showed two peaks at δ 12.3 (C_b) and 15.6 (C_a) ppm corresponding to the two methyl groups attached to the pyrazole ring. The carbon atoms of the morpholine residue, *C*—N—*C* and *C*—O—*C*, were observed at δ 43.3 and 65.9 ppm, respectively. The carbon atoms of the pyrazole moiety (C_4, C_5 and C_3, Scheme 1) were observed at δ 112.4, 142.5 and 149.5 ppm, respectively, while the *s*-triazine core carbon atoms (*N*-*C*=N, $C_{6'}$, $C_{2'}$ and $C_{4'}$) were observed at δ 162.7, 164.2 and 164.8 ppm, respectively.

In the ^{1}H NMR spectrum of the complex [Pd(BPT)Cl]ClO_4 (**2**), the protons of the four methyl groups of both pyrazole rings were observed as three singlets at δ 2.51, 2.62 and 2.74 ppm. Additionally, the protons of the methylamino (CH_3N) and methylene (CH_2)

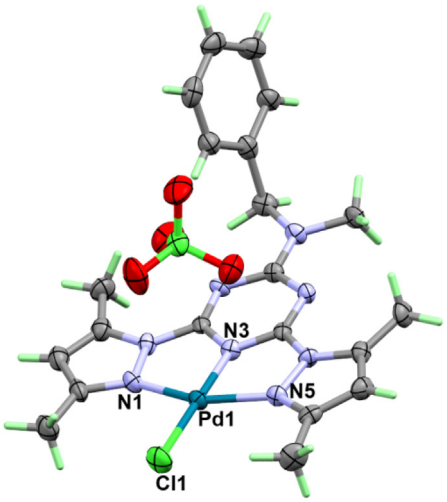

Fig. 4. X-ray structure of **2**.

groups were detected as two singlets at δ 3.29 and 5.02 ppm, respectively. While the two pyrazole protons (C*H* = C), which appeared in the free **BPT** ligand at δ 6.31 and 6.37 ppm, were slightly shifted downfield in the Pd(II) complex **2** to δ 6.64 and 6.68 ppm, respectively. In the ^{13}C NMR spectrum of **2**, the five methyl carbon atoms of the pyrazole and methylamino groups were detected at δ 12.3, 15.6 and 40.5 ppm. The methylene carbon (CH_2) was observed at δ 53.5 ppm, while the sp^2-hybridized carbon

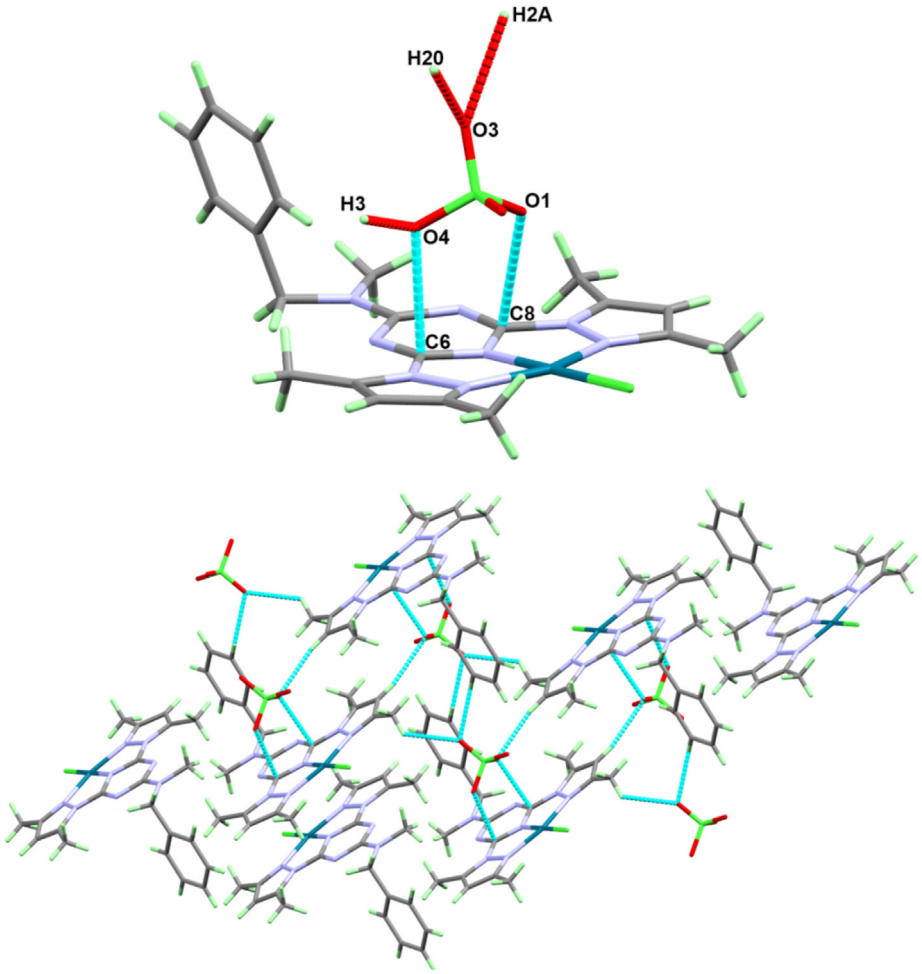

Fig. 5. Most important contacts (upper) and molecular packing through weak C—H. . .O and anion-π stacking (lower) in **2**.

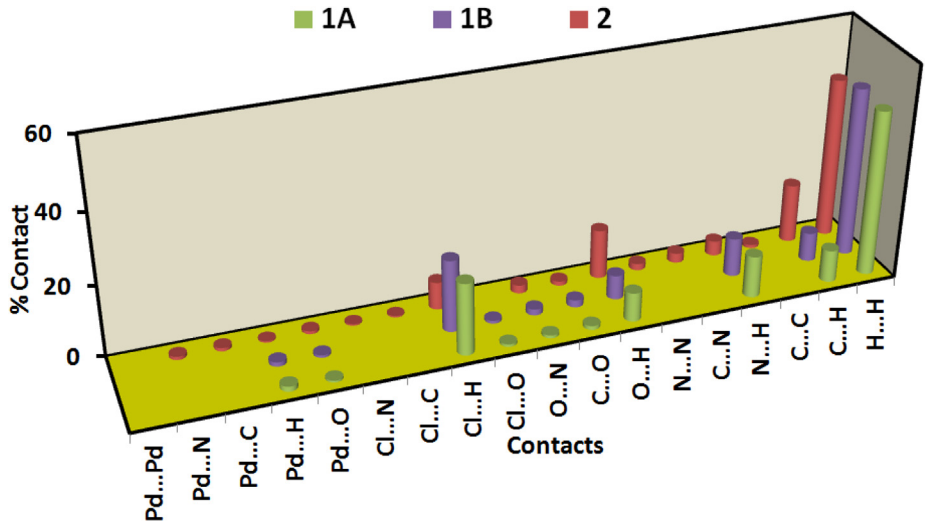

Fig. 6. Intermolecular interactions in complexes **1** and **2**.

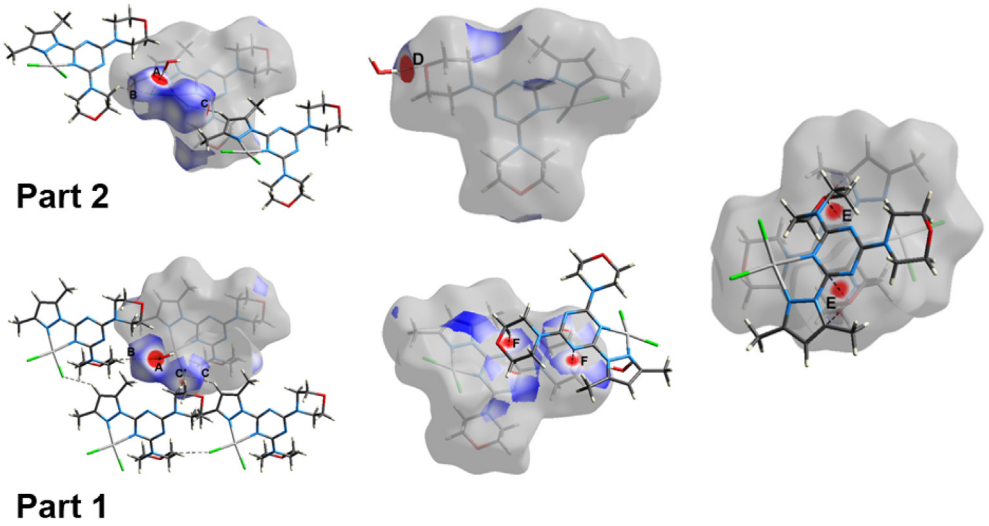

Fig. 7. The d_{norm} of the O3-H3B...Cl2 (**A**), C13-H13D...Cl2 (**B**), C3-H3...Cl1(**C**), C13B-H13A...Cl1 (**C'**) and O3-H3A...O1 (**D**) hydrogen bonds, as well as the C...O contacts (**E**) and C11B-H11D...N4 (**F**) in **1**.

atoms of the pyrazole rings, which appeared in the free **BPT** ligand at δ 111.2, 144.4 and 152.3 ppm, were slightly shifted in the Pd(II) complex **2** to δ 112.4, 145.8 and 149.5 ppm, respectively (see the Experimental section and Supplementary data for more information).

5.2. X-ray structure description

The structure of $[Pd(MPT)Cl_2].H_2O$ (**1**), with thermal ellipsoids at the 50% probability level, is shown in Fig. 2. The Pd(II) ion is coordinated with one **MPT** ligand in a bidentate mode, with Pd1-N1 (2.0199(16) Å) being slightly shorter than Pd1-N3 (2.0595(16) Å), probably due to steric hinderance between the *s*-triazine and morpholine moieties which lead to a longer Pd-N(*s*-triazine) bond than the Pd-N(pyrazole) bond. The coordination sphere of the Pd (II) ion is completed by two Pd-Cl bonds at *cis* positions, with Pd1-Cl1 and Pd1-Cl2 distances of 2.2778(5) and 2.2746(5) Å, respectively (Table 2). The Cl1-Pd1-Cl2 angle is 88.81(2)° whilst the N1-Pd1-N3 bite angle of the **MPT** ligand is 78.15(6)°. The angle between the *trans* bonds are in the range 169.91(5)° for N1-Pd1-Cl1 to 174.06(5)° for N3-Pd1-Cl2. The PdN_2Cl_2 coordination sphere shows a distorted square planar geometry. The values of the continuous shape measurements are 31.19 compared to a tetrahedron and only 0.91 compared to a square planar geometry. As a result, the coordination geometry of **1** is distorted square planar.

The crystal water molecule connects each of two $[Pd(MPT)Cl_2]$ units by O3-H3B...Cl2 and O3-H3A...O1 hydrogen bonds (Table 3), leading to the hydrogen bonded dimer shown in Fig. 3A. These dimer units are further connected with each other by C3-H3...Cl1 hydrogen bonding interactions (Fig. 3B).

In the complex $[Pd(BPT)Cl]ClO_4$ (**2**), the **BPT** ligand coordinates to the Pd(II) ion in a pincer fashion, as an *NNN*-chelate (Fig. 4). The Pd1-N3 bond distance is the shortest (1.929(5) Å) compared to the other Pd-N bonds with the pyrazolyl moieties (Pd1-N1 = 2.038(6) Å and Pd1-N5 = 2.046) Å), which is common for such a type of pincer ligand. The coordination sphere is completed by the Pd1-Cl1 bond (2.2903(18) Å) *trans* to the Pd-N interaction of the central *s*-triazine core. The angles between the *trans* bonds are 179.61(16) and 157.1 (2)° for N3-Pd1-Cl1 and N1-Pd1-N5, respectively, while the angles between the *cis* bonds are in the range 78.0(2)-102.36(16)°, suggesting a more distorted square planar geometry compared to **1**. The bite angles of the **BPT** ligand are 78.0(2) and 79.1(2)° for N3-Pd1-N1 and N1-Pd1-Cl1, respectively. The values of the continuous shape measurements are 33.00 and 2.13 compared to tetrahedral and square planar geometries. The value of 2.13 is higher than that of 0.91 for complex **1**, suggesting a more distorted square planar arrangements of the donor atoms around the Pd(II) centre than in **1**.

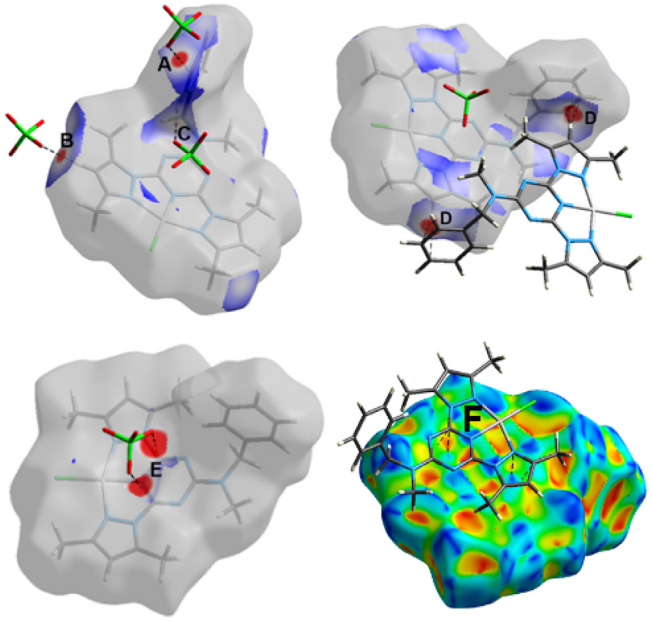

Fig. 8. The Hirshfeld d_{norm} analysis of the C20-H20...O3 (**A**), C3-H3...O4 (**B**) and C21-H21...O4 (**C**) interactions as well as the C—H...π (**D**) and anion-π stacking (**E**), as well as the shape index of the weak π-π (**F**) interactions in **2**.

Table 4
Charges at the Pd centre and coordinated ligand units.

Atom	CPX-1		Atom	CPX-2	
	MPW1PW91	**WB97XD**		**MPW1PW91**	**WB97XD**
Pd	0.2691	0.2996	Pd	0.4999	0.5200
Cl	−0.3932	−0.4091	Cl^-	−0.4460	−0.4617
Cl	−0.3798	−0.3949	ClO_4^-	−0.9445	−0.9468
MPT	0.5040	0.5043	BPT	0.8905	0.8885

Table 5
AIM topological parameters for the different Pd-N and Pd-Cl coordination interactions using the MPW1PW91 method.

Bond	ρ(r)	G(r)	V(r)	H(r)	(V(r)/G(r)	E_{int}
			Complex 1			
Pd1-N3	0.0953	0.1480	−0.1740	−0.0260	1.176	54.58
Pd1-N1	0.0884	0.1350	−0.1579	−0.0229	1.170	49.53
Pd1-Cl1	0.0819	0.1027	−0.1281	−0.0255	1.248	40.20
Pd1-Cl2	0.0822	0.1031	−0.1285	−0.0254	1.246	40.32
			Complex 2			
Pd1-N1	0.0779	0.1727	−0.1920	−0.0192	1.111	60.23
Pd1-N3	0.1283	0.1924	−0.2373	−0.0449	1.234	74.46
Pd1-N5	0.0757	0.1685	−0.1864	−0.0179	1.106	58.49
Pd1-Cl1	0.0794	0.1026	−0.1262	−0.0235	1.229	39.58

[a]H(r): Total energy density; [b]Potential (V(r)) and kinetic energy (G(r)) density.

The packing of the $[Pd(BPT)Cl]ClO_4$ complex units is controlled by weak C—H...O interactions and anion-π stacking (Table 3 and Fig. 5). The anion-π stacking occurs between the ClO_4^- anion and the carbon atoms from the *s*-triazine moiety, with C6...O4 and C8...O1 distances of 2.781(9) and 2.873(8) Å, respectively.

5.3. Hirshfeld analysis

A summary of all the contacts and their percentages in complexes **1** and **2** are shown in Fig. 6. The d_{norm} of the important contacts in complex **1** are shown in Fig. 7.

The packing of complex **1** is controlled by Cl...H (20.2%), O...H (6.8–8.1%) and N...H (10.8–11.7%) hydrogen bonds, as well as some C—H...π (8.1–9.0%) interactions and C...O contacts (1.1–2.0%). Since the studied complex comprises a disordered morpholine ring, we have two complex parts based on the disorder model; hence we analyzed all possible intermolecular interactions in both parts. Both parts showed O3-H3B...Cl2, C13-H13D...Cl2 and C3-H3...Cl1 interactions with Cl...H distances of 2.323, 2.740 and 2.563 Å, respectively. Also, short O3-H3A...O1/O3-H3A...O1B hydrogen bonds with hydrogen-acceptor distances of 1.965 and 1.798 Å were detected in the first and second parts, respectively. Interestingly, a stacked dimer *via* C4...O2 (3.173 Å) and C6...O2 (2.999 Å) short contacts between the morpholine oxygen atom from one complex unit and C atoms of the pyrazole and triazine moieties from a neighbouring complex was detected (region E). In addition, weak C13B-H13A...Cl1 and C11B-H11D...N4 interactions with donor-acceptor distances of 2.738 and 2.459 Å were observed only in the first part.

In complex **2**, all O...H contacts (13.8%) belong to weak C—H...O interactions. The C20-H20...O3, C3-H3...O4 and C21-H21...O4 interaction distances are 2.350, 2.414 and 2.547 Å, respectively. In addition, the shortest H...π contacts are C18...H11 (2.537 Å), C19...*H*11 (2.601 Å) and C17...*H*11 (2.735 Å), indicating weak aromatic C—H...π interactions (16.5%). The anion-π stacking (C...O: 1.2%) interactions occur between the perchlorate oxygen atoms and carbon atoms from the *s*-triazine moiety with C...O distances of 2.781 Å (C6...O4) and 2.873 Å (C8...O1). Also, the C...C (3.539 Å) and C...N (3.323 Å) interactions revealed the presence of weak π-π stacking between the pyrazole moieties (Fig. 8).

5.4. DFT studies

5.4.1. Natural population analysis (NPA)

The NPA analysis results of complexes **1** and **2** are shown in Table 4. The charge at the divalent palladium ion is significantly compensated by the negative charge density of the ligand groups. Its charge is reduced to 0.3 and 0.5 e in complexes **1** and **2**, respectively. The charge at the Pd(II) centre is significantly more compensated in complex **1** than **2**, possibly due to the presence of two coordinated chloride ions in **1**. The amount of electrons transferred from the two coordinated Cl^- ions is 1.2 e in **1** and 0.5 e per Cl^- ion in **2**. Also, the bidentate **MPT** ligand transferred about 0.5 e to the Pd(II) ion in **1**, while the corresponding value for the tridentate pincer ligand (**BPT**) in **2** is 0.9 e.

5.4.2. AIM topology analysis

The computed atoms in molecules topological parameters [30–38] are collected in Table 5. At a first glance, the negative H (r) and V(r)/G(r)>1 for all Pd-N and Pd-Cl bonds indicate significant covalent character for these interactions. In addition, the electron density (ρ(r)) values at the critical point of these bonds are higher for shorter bonds than longer ones. The ρ(r) values are in the range 0.0757–0.1283 a.u. It is maximum for the Pd-N(*s*-triazine) bond in complex **2**, which is the shortest one among the Pd-N bonds. In this case, the Pd-N interaction energy is the highest (74.46 kcal/mol) while the corresponding values for the other Pd-N bonds are less (49.53–60.23 kcal/mol). Good correlations were obtained between the Pd-N distances, ρ(r) and the interaction energies (Fig. 9).

5.5. Anticancer activity

5.5.1. MTT (3-(4,5-dimethyl thiazol-2yl)-2, 5-diphenyl tetrazolium bromide) assay

Complexes **1** and **2** showed significant cell growth inhibition against MDA-MB-231 and MCF-7 compared to their original ligands. It has been reported that the ligand **MPT** was completely inactive against both cell lines, whilst the **BPT** ligand showed weak

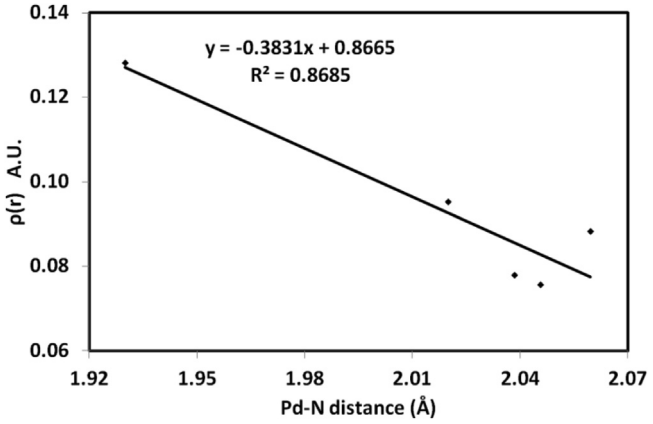

Fig. 9. Correlation between the Pd-N distances with ρ(r). A similar correlation was obtained with the interactions energies and the correlation coefficient R^2 = 0.8265 using the MPW1PW91 method.

activity against MDA-MB-231 (IC_{50} value of 50 μg/mL) and good activity against MCF-7 (IC_{50} value of 12.5 μg/mL) [17]. In our studies, complex **2** was found to be more active than complex **1**. The calculated IC_{50} values for complexes **1** and **2** were 30.5 and 13.5 μg/mL respectively against MDA-MB-231. Similarly, the calculated IC_{50} values for complexes **1** and **2** were 30.5 and 18.6 μg/mL, respectively, against MCF-7 (Fig. 10). The Pd complexes enhanced the anticancer activities against the two tested cell lines, as determined by the MTT cell viability assay. This observation is in agreement with the literature [11].

5.5.2. Cell morphology

The morphological changes of MDA-MB-231 and MCF-7 after 48 h of treatment with complex **2** were imaged using an inverted light microscope (Fig. 11) [39]. The untreated cells displayed normal cell morphology with an intact membrane and a high density of cells. However, the treated cells showed a reduction in the cell number and volume after the treatment. The cells showed apoptotic features, such as shrinkage, rounding of cells and membrane blabbing.

6. Conclusions

Two square planar Pd(II) complexes with mono- and *bis*-pyrazolyl-*s*-triazine ligands were synthesized and their structures were elucidated. In the $[Pd(MPT)Cl_2]$ (**1**) and $[Pd(BPT)Cl]ClO_4$ (**2**) complexes, the Pd(II) ion is coordinated with the **MPT** and **BPT** ligands as bidentate and tridentate chelates, respectively. DFT calculations were used to perform natural population analysis and to investigate the nature and strength of the Pd-N and Pd-Cl coordination interactions. The IC_{50} values for breast cancer cells were evaluated for complexes **1** and **2**. Both complexes showed higher activity compared to the free ligands. Complex **2** showed higher cytotoxic activity against MDA-MB-231 (IC_{50} = 13.5 μg/mL) and MCF-7 (IC_{50} = 18.6 μg/mL) compared to **1**. Finally, we propose that the

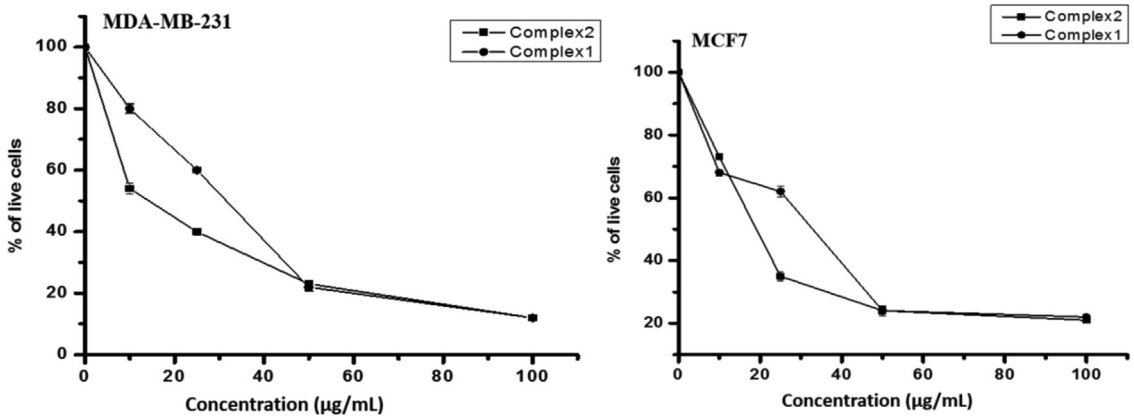

Fig. 10. Cytotoxicity of complexes **1** and **2** against MDA-MB-231 and MCF-7 after 48 h of treatment. Data are mean values of triplicates ± SD.

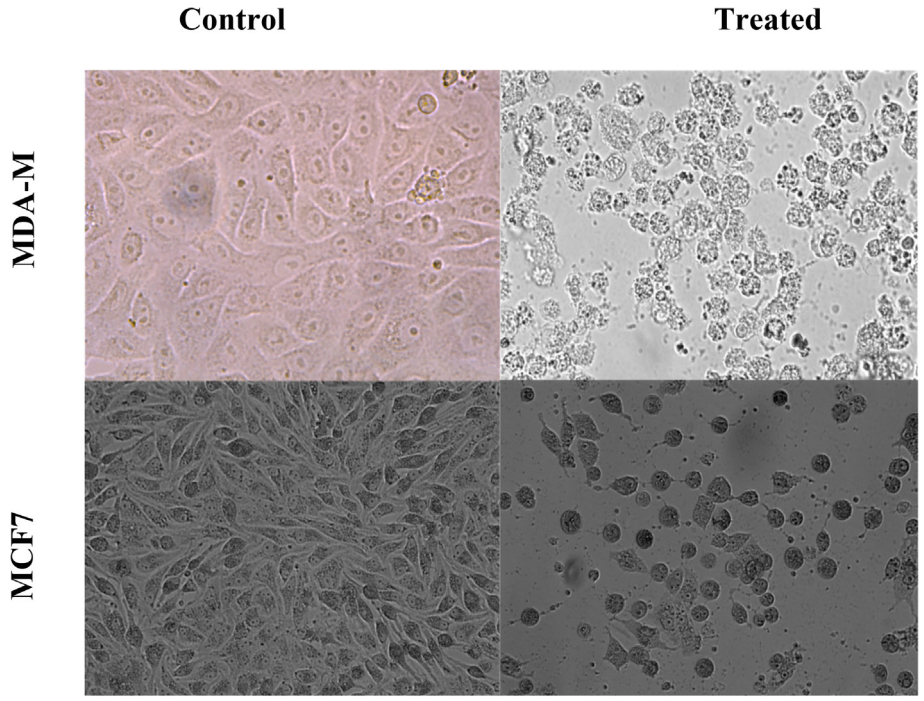

Fig. 11. Morphological changes in MDA-MB-231 and MCF-7 cells treated with 15 and 20 μg/mL of complex **2**, respectively.

inhibitory activity of these Pd(II) complexes needs further consideration for the development of anticancer agents.

Declaration of Competing Interest

The authors declare that they have no known competing financial interests or personal relationships that could have appeared to influence the work reported in this paper.

Acknowledgements

The authors would like to extend their sincere appreciation to the Deanship of Scientific Research at King Saud University for providing funding to the research group no. RGP-1441-234, Saudi Arabia.

Appendix A. Supplementary data

Supplementary data to this article can be found online at https://doi.org/10.1016/j.poly.2020.114665.

References

[1] M.J. Hannon, Pure Appl. Chem. 79 (2007) 2243–2261.
[2] (a) J. Haribabu, M.M. Tamizh, C. Balachandran, Y. Arun, N.S.P. Bhuvanesh, A. Endo, R. Karvembu, New J. Chem. 42 (2018) 10818–10832;
(b) J. Silva, A.S. Rodrigues, P.A. Videira, J. Lasri, A. Januário Charmier, A.J.L. Pombeiro, A.R. Fernandes, Inorg. Chim. Acta. 423 (2014) 156–167.
[3] I. Warad, A.F. Eftaiha, M.A. Al-Nuri, A.I. Husein, M. Assal, A. Abu-Obaid, N.N. Al-Zaqri, T. Ben Hadda, B. Hammouti, J. Mater. Environ. Sci. 4 (2013) 542–557.
[4] J.T. Hartmann, H.-P. Lipp, Expert Opin. Pharmacother. 4 (2003) 889–901.
[5] Y.-P. Ho, S.C.F. Au-Yeung, K.K.W. To, Med. Res. Rev. 23 (2003) 633–655.
[6] X. Yao, K. Panichpisal, N. Kurtzman, K. Nugent, Am. J. Med. Sci. 334 (2007) 115–124.
[7] (a) A.R. Kapdi, I.J.S. Fairlamb, Chem. Soc. Rev. 43 (2014) 4751–4777;
(b) A.M. Mansour, N.T. Abdel-Ghani, Inorg. Chim. Acta 438 (2015) 76–84.
[8] (a) L. Szucova, Z. Travnıcek, M. Zatloukal, I. Popa, Bioorg. Med. Chem. 14 (2006) 479–491;
(b) M. Nur, A.F. Huq, Coord. Chem. Rev. 316 (2016) 36–67.
[9] M. Muralisankar, S. Sujith, N.S.P. Bhuvanesh, A. Sreekanth, Polyhedron 18 (2016) 103–117.
[10] M. Muralisankar, J. Haribabu, N.S.P. Bhuvanesh, R. Karvembu, A. Sreekanth, Inorg. Chim. Acta 449 (2016) 82–95.
[11] (a) A. Kumar, A. Naaz, A.P. Prakasham, M. Kumar Gangwar, R.J. Butcher, D. Panda, P. Ghosh, ACS Omega 2 (2017) 4632–4646;
(b) S. Ray, R. Mohan, J.K. Singh, M.K. Samantaray, M.M. Shaikh, M.D. Panda, P. Ghosh, J. Am. Chem. Soc. 129 (2007) 15042–15053;
(c) N.K. Sharma, R.K. Ameta, M. Singh, Int. J. Med. Chem. 2016 (2016) 10, 9245619;
(d) E. Ulukaya, F. Ari, K. Dimas, E.I. Ikitimur, E. Guney, V.T. Yilmaz, Eur. J. Med. Chem. 46 (2011) 4957–4963.
[12] R.D. Graham, D.R. Williams, J. Inorg. Nucl. Chem. 41 (1979) 1245–1249.
[13] (a) H.L. Ng, X. Ma, E.H. Chew, W.K. Chui, J. Med. Chem. 60 (2017) 1734–1745;
(b) D.R. Shah, R.P. Modh, K.H. Chikhalia, Future Med. Chem. 6 (2014) 463–477;
(c) B. Liu, T. Sun, Z. Zhou, L. Du, Med. Chem. 5 (2015) 131–148;
(d) A. Barakat, F.F. El-Senduny, Z. Almarhoon, H.H. Al-Rasheed, F.A. Badria, A. M. Al-Majid, A. El-Faham, J. Chem. 2019 (2019) 10, 9403908;
(e) A. El-Faham, S.M. Soliman, H.A. Ghabbour, Y.A. Elnakady, T.A. Mohaya, M.R. Siddiqui, F. Albericio, J. Mol. Struct. 1125 (2016) 121–135.
[14] S.N. Mikhaylichenko, S.M. Patel, S. Dalili, A.A. Chesnyuk, V.N. Zaplishny, Tetrahedron Lett. 50 (2009) 2505–2508.
[15] (a) J.W. Tessmann, J. Buss, K.R. Begnini, L.M. Berneira, F.R. Paula, C.M.P. de Pereira, T. Collares, F.K. Seixas, Biomed. Pharmacother. 94 (2017) 37–46;
(b) M.J. Akhtar, A.A. Khan, Z. Ali, R.P. Dewangan, M. Rafi, M.Q. Hassan, M.S. Akhtar, A.A. Siddiqui, S. Partap, S. Pasha, Bioorg. Chem. 78 (2018) 158–169.
[16] (a) W. Yan, Y. Zhao, J. He, Mol. Med. Rep. 18 (2018) 4175–4184;
(b) L. Moreno, J. Quiroga, R. Abonia, J.R. Prada, B. Insuasty, Molecules 23 (2018) 1956;
(c) F. Manna, F. Chimenti, R. Fioravanti, A. Bolasco, D. Secci, P. Chimenti, C. Ferlini, G. Scambia, Bioorg. Med. Chem. Lett. 15 (2005) 4632–4635.
[17] M. Farooq, A. Sharma, Z. Almarhoon, A. Al-Dhfyan, A. El-Faham, N. Abu Taha, M.A.M. Wadaan, B.G. de la Torre, F. Albericio, Bioorg. Chem. 87 (2019) 457–464.
[18] A. El-Faham, M. Farooq, Z. Almarhoon, R. Abd Alhameed, M. A.M. Wadaan, B. G. de la Torre, F. Albericio, Bioorg. Chem., 94 (2020) 103397.
[19] (a) S.M. Soliman, S.E. Elsilk, A. El-Faham, Inorg. Chim. Acta 508 (2020) 119627;
(b) S.M. Soliman, S.E. Elsilk, A. El-Faham, Inorg. Chim. Acta 510 (2020) 119753.
[20] S.M. Soliman, J.H. Albering, E.N. Sholkamy, A. El-Faham, Appl. Organomet. Chem. 34 (2020) e5603.
[21] S.M. Soliman, Z. Almarhoon, E.N. Sholkamy, A. El-Faham, J. Mol. Struct. 1195 (2019) 315–322.
[22] (a) A. Sharma, H. Ghabbour, S.T. Khan, G. Beatriz, F. Albericio, A. El-Faham, J. Mol. Str. 1145 (2017) 244;
(b) C. Yang, W.-T. Wong, Y. Cui, Y. Yang, Sci. China Ser. B 44 (2001) 80–92.
[23] (a) Z. Otwinowski, W. Minor, Processing of X-ray Diffraction Data Collected in Oscillation Mode, Academic Press, New York, 1997, pp. 307–326;
(b) C. W. Carter, J. Sweet, In Methods in Enzymology, Macromolecular Crystallography, Part A, Eds.; Academic Press: New York, USA, 276 (1997) 307–326.;
(c) G.M. Sheldrick, Acta Cryst., C 71 (2015) 3–8;
(d) G.M. Sheldrick, SADABS – Bruker Nonius Scaling and Absorption Correction, Bruker AXS Inc, Madison, Wisconsin, USA, 2012.
[24] (a) M. J. Turner, J. J. McKinnon, S. K. Wolff, D. J. Grimwood, P. R. Spackman, D. Jayatilaka, M. A. Spackman, Crystal Explorer 17 (2017) University of Western Australia; http://hirshfeldsurface.net.;
(b) F.L. Hirshfeld, Theor. Chim. Acta 44 (1977) 129–138;
(c) M.A. Spackman, D. Jayatilaka, Cryst. Eng. Comm. 11 (2009) 19–32;
(d) M.A. Spackman, J.J. McKinnon, Cryst. Eng. Commun. 4 (2002) 378–392;
(e) J. Bernstein, R.E. Davis, L. Shimoni, N.-L. Chang, Angew. Chem. Int. Ed. 34 (1995) 1555–1573;
(f) J.J. McKinnon, D. Jayatilaka, M.A. Spackman, Chem. Comm. (2007) 3814–3816.
[25] M.J. Frisch, G.W. Trucks, H.B. Schlegel, G.E. Scuseria, M.A. Robb, J.R. Cheeseman, G. Scalmani, V. Barone, B. Mennucci, G.A. Petersson, H. Nakatsuji, M. Caricato, X. Li, H.P. Hratchian, A.F. Izmaylov, J. Bloino, G. Zheng, J.L. Sonnenberg, M. Hada, M. Ehara, K. Toyota, R. Fukuda, J. Hasegawa, M. Ishida, T. Nakajima, Y. Honda, O. Kitao, H. Nakai, T. Vreven, J.A. Montgomery, Jr., J.E. Peralta, F. Ogliaro, M. Bearpark, J.J. Heyd, E. Brothers, K.N. Kudin, V.N. Staroverov, R. Kobayashi, J. Normand, K. Raghavachari, A. Rendell, J.C. Burant, S.S. Iyengar, J. Tomasi, M. Cossi, N. Rega, J.M. Millam, M. Klene, J.E. Knox, J.B. Cross, V. Bakken, C. Adamo, J. Jaramillo, R. Gomperts, R.E. Stratmann, O. Yazyev, A.J. Austin, R. Cammi, C. Pomelli, J.W. Ochterski, R.L. Martin, K. Morokuma, V.G. Zakrzewski, G.A. Voth, P. Salvador, J.J. Dannenberg, S. Dapprich, A.D. Daniels, O. Farkas, J.B. Foresman, J.V. Ortiz, J. Cioslowski, D.J. Fox, Gaussian, Inc., Wallingford CT, (2009).
[26] (a) J.D. Chai, M. Head-Gordon, Phys. Chem. Chem. Phys. 10 (2008) 6615–6620;
(b) C. Adamo, V. Barone, J. Chem. Phys. 108 (1998) 664–675.
[27] (a) https://bse.pnl.gov/bse/portal.;
(b) D. Feller, J. Comp. Chem. 17 (1996) 1571–1586;
(c) K.L. Schuchardt, B.T. Didier, T. Elsethagen, L. Sun, V. Gurumoorthi, J. Chase, J. Li, T.L. Windus, J. Chem. Inf. Model. 47 (2007) 1045–1052.
[28] NBO Version 3.1, E.D. Glendening, A.E. Reed, J.E. Carpenter, F. Weinhold, NBO Version 3.1, CI, University of Wisconsin, Madison, (1998).
[29] T. Lu, F. Chen, J. Comput. Chem. 33 (2012) 580–592.
[30] R.F.W. Bader, Atoms in Molecules: A Quantum Theory, Oxford University Press, Oxford, U.K., (1990).
[31] C.F. Matta, J. Hernandez-Trujillo, T.-H. Tang, R.F.W. Bader, Chem. Eur. J. 9 (2003) 1940–1951.
[32] S.J. Grabowski, A. Pfitzner, M. Zabel, A.T. Dubis, M. Palusiak, J. Phys. Chem., B 108 (2004) 1831–1837.
[33] C.F. Matta, N. Castillo, R.J. Boyd, J. Phys. Chem. A 109 (2005) 3681–13669.
[34] A.M. Pendás, E. Francisco, M.A. Blanco, C. Gatti, Chem. Eur. J. 13 (2007) 9362–9371.
[35] M.F. Bobrov, G.V. Popova, V.G. Tsirelson, Russ. J. Phys. Chem. 80 (2006) 584–590.
[36] (a) C. Gatti, Z. Kristallogr. 220 (2005) 399–457;
(b) G.V. Gibbs, R.T. Downs, D.F. Cox, N.L. Ross, M.B. Boisen, K.M. Rosso, J. Phys. Chem. A 112 (2008) 3693–3699.
[37] E. Espinosa, E. Molins, C. Lecomte, Chem. Phys. Lett. 285 (1998) 170–173.
[38] D. Cremer, E. Kraka, Angew. Chem., Int. Ed. Engl. 23 (1984) 627–628.
[39] N. Abutaha, F.A. Nasr, A.Z. Mohammed, A. Semlali, F.A. Al-Mekhlafi, M.A. Wadaan, Mol. Biol. Rep 46 (2019) 2187–2196.